

SUPPLEMENTAL DATA

δ -Tocopherol Effect on Endocytosis and its Combination with Enzyme Replacement Therapy for Lysosomal Disorders: a New Type of Drug Interaction?

*Rachel L. Manthe[†], Jeffrey A. Rappaport[†], Yan Long, Melani Solomon, Vinay Veluvolu, Michael
Hildreth, Dencho Gugutkov, Juan Marugan, Wei Zheng, and Silvia Muro**

R.L.M., J.A.R., V.V. & M.H.: Fischell Department of Bioengineering, University of Maryland,
College Park, MD 20742, USA

Y.L., J.M. & W.Z.: National Center for Advancing Translational Sciences, National Institutes of
Health, Bethesda, MD 20892, USA

D.G. & S.M.: Institute for Bioengineering of Catalonia (IBEC) of the Barcelona Institute of
Science and Technology (BIST), Barcelona, 02028, Spain

S.M.: Institution of Catalonia for Research and Advanced Studies (ICREA), Barcelona, 08010,
Spain

M.S. & S.M.: Institute for Bioscience and Biotechnology Research, University of Maryland,
College Park, MD 20742, USA

This work was supported by the National Institutes of Health [Grant R01 HL98416], Spanish Ministry of Economy and Competitiveness - MINECO/FEDER project SEV-2014-0425, Spanish Ministry of Science, Innovation and University - MINECO/EXPLORA project SAF2017-91909-EXP and MINECO/RETOS project RTI2018-101034-B-I00, and CERCA Program of the Generalitat de Catalunya awarded to S.M.; National Science Foundation Graduate Research Fellowship [DGE-0750616], University of Maryland Flagship Fellowship, the National Institutes of Health Ruth L. Kirschstein Pre-Doctoral Fellowship [F31-HL128121] awarded to R.L.M.; Howard Hughes Medical Institute Fellowship Program under the University of Maryland Undergraduate Science Education Program awarded to J.A.R.; and by Intramural Research Program of the National Institutes of Health [National Center for Advancing Translational Sciences] awarded to W.Z.

[†]These authors contributed equally to this article.

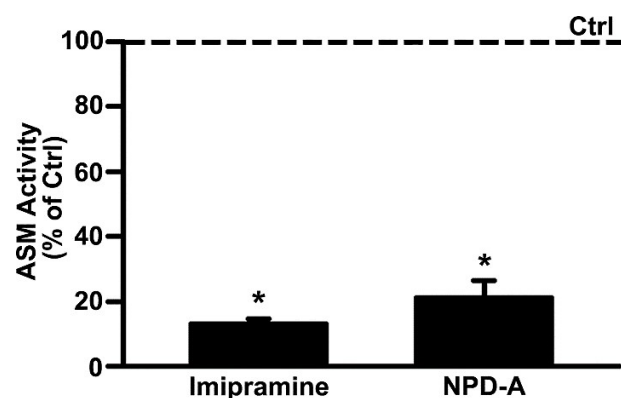


Figure S1. Endogenous ASM activity in pharmacological and genetic NPD-A cell models. ASM activity was determined in imipramine-diseased endothelial cells and NPD-A patient fibroblasts using an artificial substrate and measuring the resulting fluorescent product in a plate reader (see **Methods**). Data were normalized to control endothelial cells or wild-type fibroblasts, respectively (horizontal dashed line). Data are mean \pm SEM ($n \geq 4$ independent wells). *Comparison to control cells ($p < 0.05$ by Student's *t*-test).

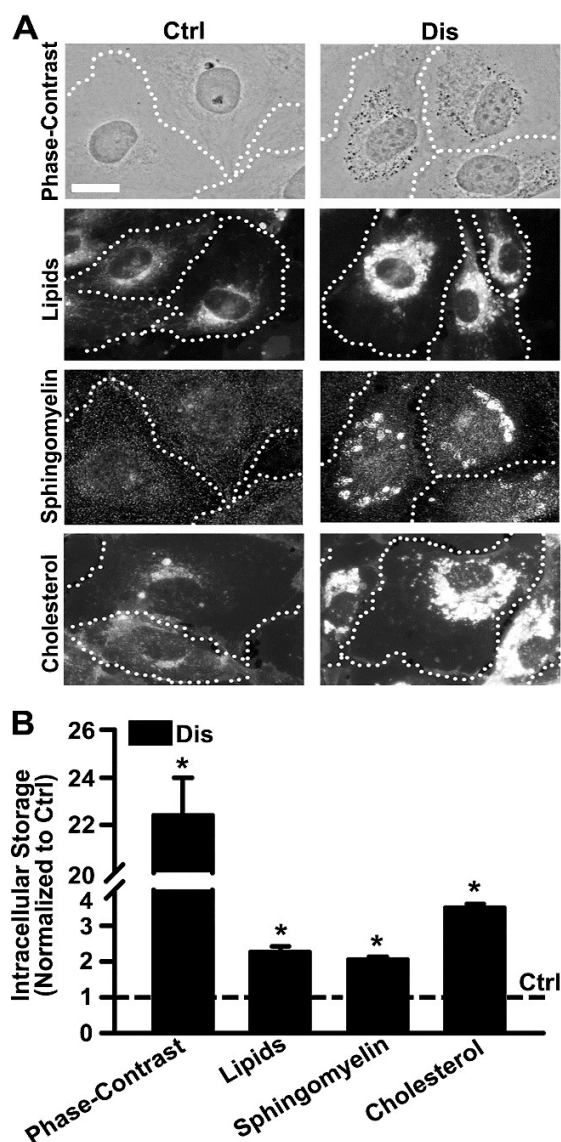


Figure S2. Induction of lipid storage in endothelial cells. (A) Microscopy of control (Ctrl) vs. imipramine-diseased endothelial cells (Dis). Dark-refringent storage compartments were visible by phase-contrast, and cells were additionally stained with fluorescent Nile Red to label lipids, lysenin to label sphingomyelin, or filipin to label cholesterol. Dotted lines mark the cell borders, as observed by phase-contrast. Scale bar = 10 μ m. (B) The mean fluorescence intensity of markers in (A) was quantified within a 3 μ m-perinuclear region, the background fluorescence (cell periphery) was subtracted, and data were normalized to control cells (horizontal dashed line). The number of dark-refringent storage compartments was quantified using phase-contrast images and also normalized to control cells. Data are mean \pm SEM ($n \geq 4$ independent wells). *Comparison to control cells ($p < 0.05$ by Student's t -test).

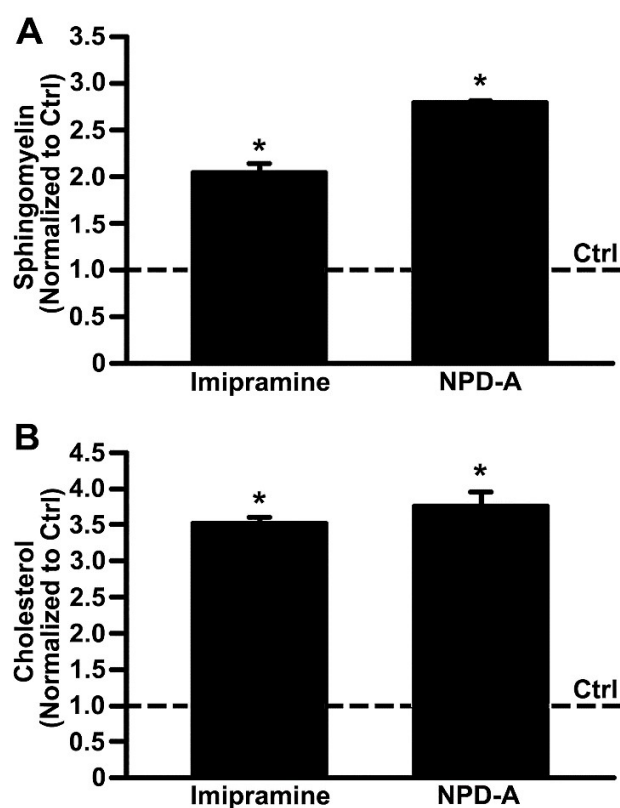


Figure S3. Sphingomyelin and cholesterol storage in pharmacological and genetic NPD-A cell models. Control and imipramine-diseased endothelial cells were stained with fluorescent lysenin or filipin to label sphingomyelin or cholesterol, respectively. Alternatively, sphingomyelin was labeled with fluorescent BODIPY-FL- C_{12} -sphingomyelin in wild-type and NPD-A patient fibroblasts, and filipin was used to label cholesterol in these cells. The mean fluorescence intensity of (A) sphingomyelin and (B) cholesterol was quantified within a 3 μ m-perinuclear region, the background fluorescence (cell periphery) was subtracted, and data were normalized to control cells (horizontal dashed line). Data are mean \pm SEM ($n \geq 4$ independent wells). *Comparison to control cells ($p < 0.05$ by Student's t -test).

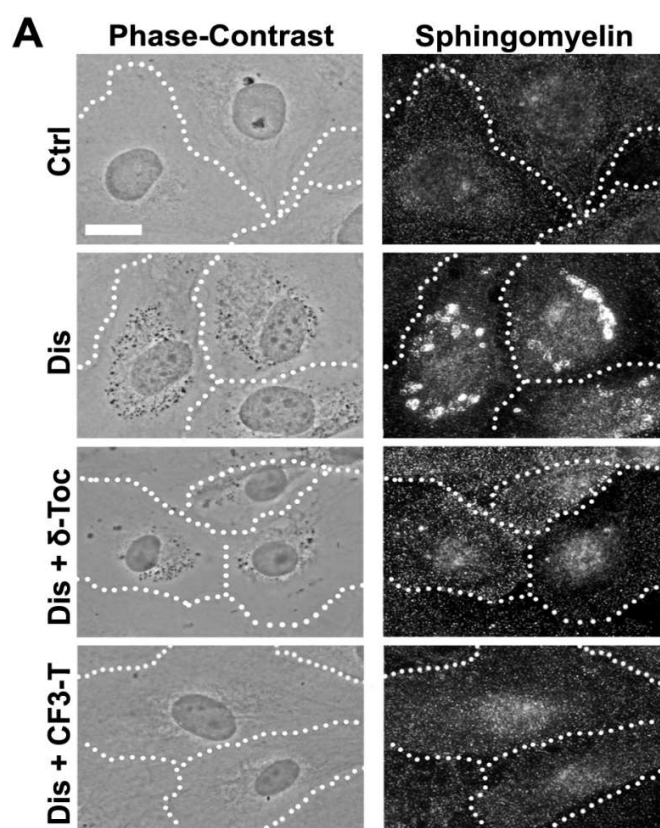


Figure S4. Micrographs of the effect of tocopherols on sphingomyelin storage in diseased endothelial cells. Phase-contrast and fluorescence microscopy images showing sphingomyelin accumulation (lysenin-positive) in control (Ctrl) vs. imipramine-diseased endothelial cells (Dis) after 48 h incubation in the absence or presence of 40 μ M δ -tocopherol (δ -Toc) or 20 μ M CF3-T. Dotted lines mark the cell borders, as observed by phase-contrast. Scale bar = 10 μ m.

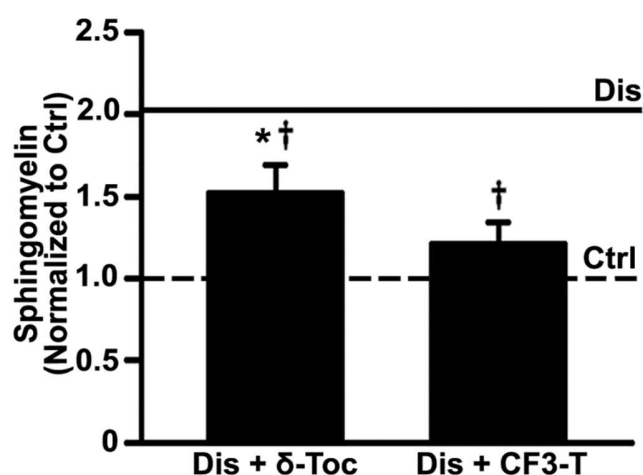


Figure S5. Reduction of sphingomyelin by tocopherols in diseased endothelial cells. Sphingomyelin was stained in imipramine-diseased endothelial cells (Dis) with fluorescent lysenin, 1 h after a 48 h treatment with 40 μ M δ -tocopherol or 20 μ M CF3-T. Sphingomyelin was then quantified as described in **Figure 1** and normalized to untreated control cells (horizontal dashed line) or untreated diseased cells (horizontal solid line). Data are mean \pm SEM ($n \geq 4$ independent wells). *Comparison to untreated control cells; †comparison to untreated diseased cells indicated by the horizontal solid line ($p < 0.05$ by Student's *t*-test).

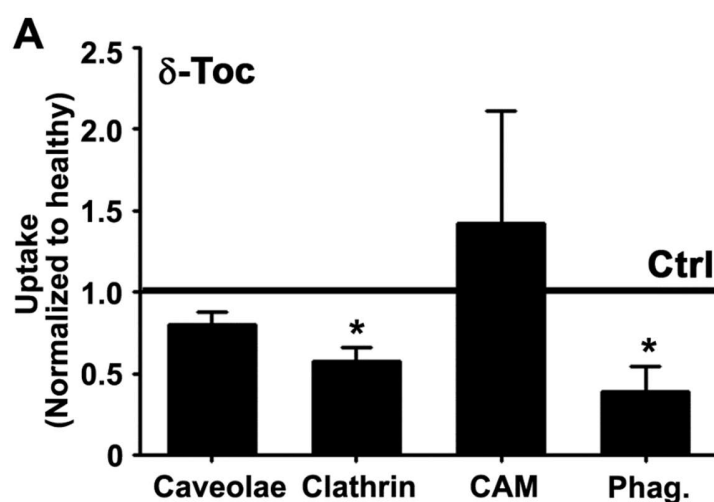


Figure S6. Effect of δ -tocopherol on receptor-mediated uptake in control endothelial cells.

Control endothelial cells (Ctrl) were treated for 48 h with 40 μ M δ -tocopherol, then incubated for 3 h with fluorescent ligands of individual endocytic pathways. Ligands were cholera toxin B (CTB; caveolae-mediated endocytosis), transferrin (Tf; clathrin-mediated endocytosis), 100 nm polymer nanocarriers targeted to ICAM-1 (anti-ICAM NCs; CAM-mediated endocytosis), and 1 μ m IgG-coated microparticles (phagocytosis; Phag.). Thereafter, cells were washed, fixed, and cell-surface bound counterparts were immunostained with antibodies fluorescently-labeled in a different color to distinguish internalized vs. surface-bound ligands (see **Methods**). Uptake data are normalized to control cells (horizontal solid line). Data are mean \pm SEM ($n \geq 4$ independent wells). *Comparison to control cells ($p < 0.05$ by Student's t -test).

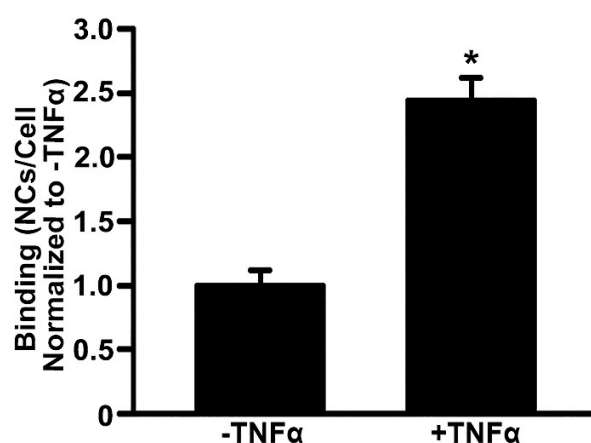


Figure S7. Effect of TNF α on anti-ICAM NC binding to diseased endothelial cells. Imipramine-diseased endothelial cells (Dis) were incubated overnight with control medium (-TNF α) or medium containing TNF α . Then, cells were incubated for 3 h with fluorescent anti-ICAM NCs, washed, fixed, and imaged by microscopy as described in **Figure 3**. Binding data are the fluorescent area of total cell-associated NCs normalized to control medium (-TNF α). Data are mean \pm SEM ($n \geq 4$ independent wells). *Comparison to -TNF α cells ($p < 0.05$ by Student's t -test).

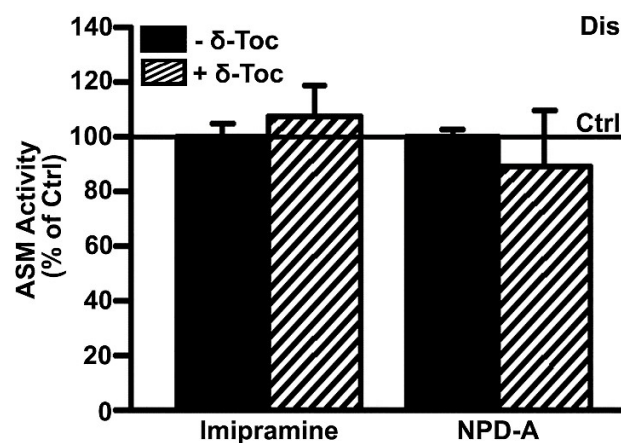


Figure S8. Effect of δ -tocopherol on endogenous ASM activity in pharmacological and genetic NPD-A cell models. The activity of endogenous ASM was measured in imipramine-diseased endothelial cells or NPD-A fibroblasts treated for 48 h with 40 μ M δ -tocopherol as described in **Figure 6**. Data are normalized to untreated diseased endothelial cells or NPD-A fibroblasts (horizontal solid line). Data are mean \pm SEM ($n \geq 4$ independent wells). No statistical significance was found.

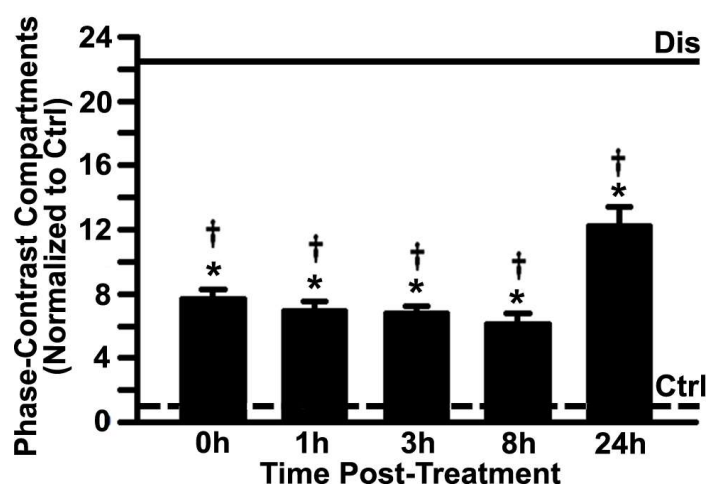


Figure S9. Effect of δ -tocopherol on dark-refractive storage compartments in diseased endothelial cells. Control (Ctrl) and imipramine-diseased endothelial cells (Dis) were incubated in fresh medium for 1-24 h after removal of 40 μ M δ -tocopherol. Cells were washed, fixed, and the number of dark-refractive storage compartments was visualized by phase-contrast, quantified as described in **Figure S2**, and normalized to control cells (horizontal dashed line). Untreated diseased cells are shown as a horizontal solid line. Data are mean \pm SEM ($n \geq 4$ independent wells). *Comparison to untreated control cells; †comparison to untreated diseased cells ($p < 0.05$ by Student's t -test).

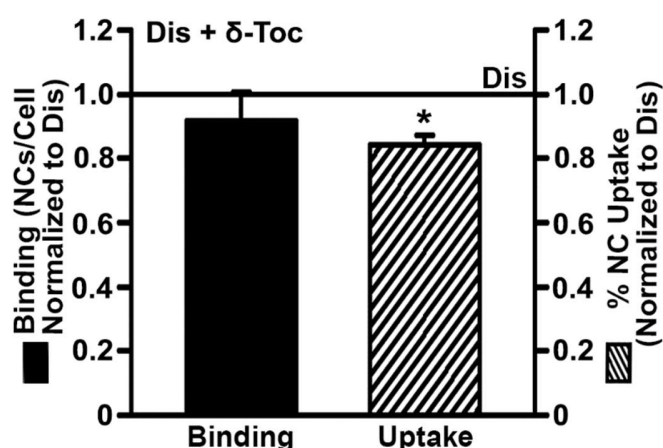


Figure S10. Anti-ICAM NC binding and uptake in diseased endothelial cells after δ -tocopherol removal. Imipramine-diseased endothelial cells (Dis) treated for 48 h with 40 μ M δ -tocopherol were activated overnight with TNF α to mimic inflammation. Cells were then incubated for 3 h with fluorescent anti-ICAM NCs 5 h after removal of δ -tocopherol. Cells were washed, fixed, immunostained, and imaged by microscopy as described in **Figure 3**. Binding was quantified as total cell-associated fluorescent NCs, while NC uptake represents internalized NCs expressed as a percentage of the total cell-associated NCs. Data were normalized to untreated diseased cells (horizontal solid line). Data are mean \pm SEM ($n \geq 4$ independent wells). *Comparison to untreated diseased cells ($p < 0.05$ by Student's t -test).